Journal of the European Ceramic Society **6** (1990) 331–337

Influence of Powder Characteristics on Impact Damage in SiC-Whisker/Si_3N_4 Composites

Yoshio Akimune

Materials Research Laboratory, Central Engineering Laboratories, Nissan Motor Co. Ltd, 1 Natsushima-cho, Yokosuka 237, Japan

(Received 29 January 1990; accepted 22 June 1990)

Abstract

The spherical impact damage of two SiC-whisker/silicon nitride matrix composites was investigated. Both exhibited elastic response and Hertzian cone crack initiation when the projectile impact velocity exceeded a critical velocity. The composite prepared from nitrided silicon powder exhibited a higher resistance to crack initiation and strength degradation than that prepared using Si_3N_4 from thermally decomposed $Si(NH)_2$ powder. This was because the higher oxygen content and lower free carbon content yield glass and a deformable microstructure more able to dissipate impact energy.

Die Schädigung zweier SiC-Whisker/Si_3N_4-Matrix Verbundwerkstoffe durch Aufprall kugelförmiger Teilchen wurde untersucht. Beide zeigten ein elastisches Verhalten und die Ausbildung Hertz'scher Risse wenn die Projektilgeschwindigkeit einen kritischen Wert überschritt. Der aus nitridiertem Siliziumpulver hergestellte Werkstoff war gegenüber der Rißbildung widerstandsfähiger und zeigte einen geringeren Festigkeitsabfall als der Werkstoff bei dem durch thermische Zersetzung von $Si(NH)_2$ Pulvern hergestelltes Si_3N_4 verwendet wurde. Der Grund für dieses Verhalten lag an einem höheren Sauerstoffgehalt und einem niedrigeren Gehalt an freiem Kohlenstoff was zur Bildung von Glas und einem verformbaren, die Energie des Aufpralls besser ableitenden Gefüge führte.

On a étudié l'endommagement par impact sphérique de deux composites à matrice nitrure de silicium renforçée par des whiskers de carbure de silicium. Les deux échantillons présentent un comportement élastique et-une initiation de fissuration en cône Hertzien lorsque la vitesse d'impact du projectile dépasse une valeur critique. Le composite préparé à partier de poudre de silicium nitrurée présente une résistance à la propagation des fissures plus élevée que celui élaboré à partir de Si_3N_4 issu de la décomposition thermique de poudre $Si(NH)_2$. Ceci s'explique par une teneur en oxygène plus élevée et une teneur en carbone plus basse dans la phase vitreuse et par une microstructure déformable, plus apte à dissiper l'énergie d'impact.

1 Introduction

Silicon nitride is a prime candidate material for heat engine components because of its high strength, thermal resistance, and modest fracture toughness.[1] However, the demand exists for increasing fracture toughnesses for anticipated applications in gas turbine components.[2] Reinforcement of silicon nitride by a SiC-whisker dispersion has been reported to improve both the fracture toughness and strength of silicon nitride composites,[3–5] although Li and Bradt[6] indicate the residual stress distribution is not a favorable one. The mechanical properties of these composites depend on the whisker shapes, length to diameter ratio and other characteristics.

It is well known, however, that the properties of silicon nitride composites are also related to the sintering behavior and the powder characteristics of the silicon nitride matrix.[7,8] For these reasons, it is anticipated that the silicon nitride powder characteristics will influence the mechanical properties of SiC-whisker/silicon nitride composites.

Impact damage is a serious problem for ceramics utilized as turbine components.[9–13] Even with fiber- or whisker-reinforced composites, there exists the possibility for damage to occur from particle impact and/or point indentation and there have been recent

Journal of the European Ceramic Society 0955-2219/90/$3.50

studies considering the practical use of ceramic composites for impact damages.[11-14] However, before ceramic composites can be practically applied as engine components, additional impact damage studies must be conducted in parallel with the studies already completed on their microstructural development.

This paper reports a study of the mechanical properties of two hot-pressed 20 vol.% SiC-whisker/silicon nitride matrix ceramic composites prepared using different types of silicon nitride powders. Impact tests were conducted and the strength degradation of these composites was examined at room temperature. The relationship between the mechanical properties of these two ceramic composites and their microstructures, as produced by different Si_3N_4 powder additions, was then studied by means of scanning electron microscopy (SEM) and transmission electron microscopy (TEM).

2 Experimental Procedures

2.1 Materials

Two types of commercially produced silicon nitride (Si_3N_4) powders and one kind of SiC-whisker (supplied by Tateho Chemical Industries Co. Ltd, Akoh, Hyougo, Japan) were used. One powder was made using the silicon nitridation method (supplied by W. C. Starck, PO Box 2540, D-3380 Goslar, FRG) and the other by means of $Si(NH)_2$ thermal decomposition (E10, supplied by Ube Industries Ltd, 1-12-32 Akasaka, Tokyo, Japan). Chemical compositions and properties of the two powders and the one whisker-type compound are listed in Table 1. Each Si_3N_4 powder and 20 vol.% of the SiC-whiskers were mixed with 10 wt% yttria (Cerac: 99·9% pure, particle size 325 mesh under) and 5 wt% alumina (Alcoa: 99·5% pure, particle size 325 mesh under) in a ball mill using ethanol as the vehicle. After ball-milling (Chuuou Chem. & Engineering Co.: 2·4 liters) for 24 h, the slurry was dried in a rotary evaporator and sieved to $<210\,\mu m$. The mixtures were then separately hot-pressed (Shimazu Co. Ltd.: VHL18/15PRS) into 50 × 40 × 6 mm plates at a pressure of 30 MPa under 0·1 MPa of N_2 in a BN-coated graphite mold for 1 h at 1840°C (heating and cooling speed: 20°C/min). The microstructures of SiC-whisker/Si_3N_4 composites were examined using transmission electron microscopy (Hitachi Co., H-800).

Table 1. Properties of Si_3N_4 powder and SiC-whisker

Properties	*Silicon nitride powder*		*SiC-whisker 1-0·7S*
	LC10	*E10*	
Chemical composition (wt%)			
N	38·43	>38	—
O	1·96	1·27	0·45
C	0·17	0·30	0·20
Al	0·05	0·05	0·29
Ca	0·01	0·05	0·14
Fe	0·01	0·10	0·04
Mg	—	—	0·11
Crystallographic structure	>95wt% α-Si_3N_4	>95% α-Si_3N_4	β-SiC
Diameter (μm)	0·5	0·5	0·78
Length (μm)	—	—	20–200
Specific density (g/cm^3)	3·18	3·18	3·18
Surface area (m^2/g)	14·6	10·3	—

The hot-pressed plates were first ground to eliminate the surface graphite layer and then diamond sawed (average particle size: 180 μm) into 4 × 3 × 40 mm specimens for subsequent mechanical testing. Impact test specimens (6 × 3 × 50 mm) were polished using two grades of diamond paste (6 and 3 μm) to remove the machining damage from the surface layer and produce mirror-like flat and parallel surfaces. A four-point bending test (inner span: 10 mm; outer span: 30 mm) with the crack plane parallel to the hot-press direction and at a crosshead speed of 0·5 mm/min was used to measure bending strength (ten specimens). The results were analyzed using Weibull statistics.[15] Fracture toughness (15 measurements) was estimated by the indentation method,[16] Young's modulus (five specimens) by resonance and the hardness (15 measurements) with a Vickers indenter at a 300-g test load.

2.2 Impact test

For the impact test, a partially stabilized zirconia (SZP) sphere (1·0 mm in diameter, supplied by Tosoh Co. Ltd, 1-7-7 Akasaka, Japan) was shot into the specimen parallel to the hot-pressing direction using a He gas pistol at room temperature.[12,13] The impact apparatus is shown in Fig. 1. The PSZ sphere was attached to the top of a plastic sabot with a small magnet. The sabot was set in the pistol of the

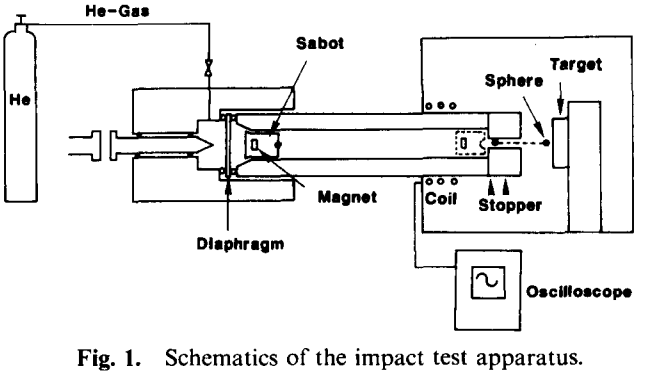

Fig. 1. Schematics of the impact test apparatus.

apparatus after the gas pressure from an He gas cylinder had risen to a specified level in the chamber. The diaphragm was then punctured by a needle, releasing the gas toward the pistol. The sabot was driven toward the end of the steel pipe at a rate dependent on the volume of gas released. At the end of the pipe, the motion of the sabot was halted, ejecting the PSZ sphere toward the target. The velocity of the sabot (80–380 m/s), including the PSZ sphere, was analyzed by three electromagnetic detectors aligned coaxially with the pistol to measure flight time. Only a single impact was made for each sabot firing. The velocity was determined for each firing based on the time-of-flight principle. The velocity was assumed equal to that of the ejected sphere at short range.

2.3 Post-impact evaluation

After the impact test, surface damage to the two types of SiC-whisker/Si_3N_4 composites was investigated using both optical microscopy and SEM. Crater depths and diameters were measured by profilometry. Post-impact bending strengths were measured by the four-point bending test (inner span: 10 mm; outer span: 30 mm) at a 0·5 mm/min crosshead speed. Fracture surfaces were also examined using optical microscopy and/or SEM.

3 Results and Discussion

3.1 Mechanical properties and microstructures

Table 2 summarizes the mechanical properties of the two 20 vol.% SiC-whisker/silicon nitride composites (SiC-W/SN). The SiC-W/SN(A) made from $Si(NH)_2$ thermal decomposition powder and the SiC-W/SN(B) made from silicon nitridation powder both had densities equal to or greater than 98% of theoretical density. The addition of the SiC-whiskers probably introduced some low density materials such as SiO_2 and/or pores, which in turn resulted in a slightly decreased composite density. The Young's modulus for the composite with the thermally decomposed $Si(NH)_2$ powder (SiC-W/SN(A)) shows a higher value than that for the composite SiC-W/SN nitridized silicon powder (SiC-W/SN(B)). Hardness values of SiC-W/SN(A) are also higher than the hardness of SiC-W/SN(B). These Young's modulus and hardness differences reflect differences related to microstructural differences in the two composite materials caused by the choice of starting Si_3N_4 powders. According to these Young's modulus and hardnesses the SiC-W/SN(A) composite yields a more rigid and harder microstructure than that of the SiC-W/SN(B) composite, although their densities are essentially the same.

Table 2. Mechanical properties

Properties	*E10 SiC-W/SN (A)*	*LC10 SiC-W/SN (B)*	*PSZ sphere*
Relative density (%TD)	98	98	>99
Crystal phase	β-SN β-SiC	β-SN β-SiC	TZP
Bend strength (MPa)[a]	1 145 ± 71	950 ± 40	1 120
Weibull modulus	19·1	29·0	—
K_{IC}(MPa m$^{1/2}$)[b]	6·0 ± 0·2	6·0 ± 0·2	7·5
Young's modulus (GPa)	315 ± 4	298 ± 4	200
Hardness (GPa)	18·7 ± 0·7	16·9 ± 0·5	12·5
Ht/*Hp*	1·50	1·35	—

[a] Four point bending test.
[b] Indentation.[16]

The fracture toughness values (K_{IC}) are also the same, but the bending strengths exhibit a large difference. Figure 2(A) and (B) show cross-sectional microstructures of the specimens broken in the four-point bending test. The grains of SiC-W/SN(A) are needle-like and the fracture path is inter-granular, which results in moderate fracture toughness. Similarly, SiC-W/SN(B) also exhibits needle-like grains (1–3 μm × 10 μm) which are much larger than those of SiC-W/SN(A) (0·5–1·5 μm × 5 μm). Both composites display the same fracture toughness values, which indicates they possess similar toughening attributes despite the difference in their β-Si_3N_4 grain sizes. Table 2 lists the Weibull moduli and the bending strengths, which show that SiC-W/SN(B) has a higher Weibull modulus, but lower strength level than that of SiC-W/SN(A). Through the addition of SiC-whiskers, the critical flaw size for the SiC-W/SN(B) composites converges, which results in a higher Weibull modulus.[7] Composite (B) exhibits a lower strength, indicative of the large β-Si_3N_4 grains.

The microstructures of the SiC-W/SN(A) and (B) composites were also observed, as shown in Fig. 3(A) and (B), using TEM. SiC-whiskers are observed with β-Si_3N_4 grains and a glassy phase. The grain sizes of the β-Si_3N_4 in SiC-W/SN(A) are smaller than those of SiC-W/SN(B). Although not readily observed, a glassy layer is believed to encompass the SiC-whiskers and to contain a combination of the SiC-whisker and Si_3N_4 grains.[17] The SiC-whisker additions are more effective in giving a rigid microstructure to SiC-W/SN(A) than to SiC-W/SN(B). This rigid microstructure is a combination of small silicon nitride grains, SiC-whiskers and glassy interfacial films between the SiC-whiskers and silicon nitride grains.[18]

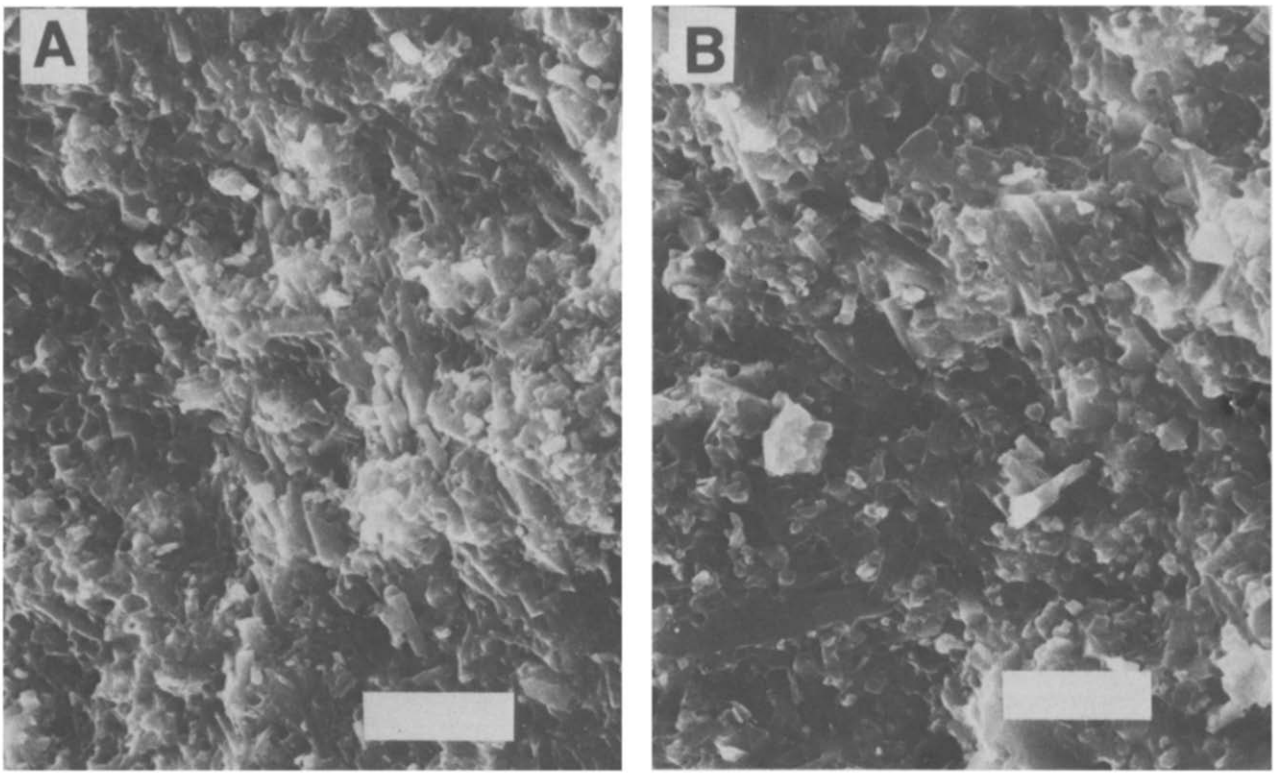

Fig. 2. Scanning electron micrographs of fracture surfaces of the SiC-W/SN composites (bar = 5 μm). (A) SiC-W/SN(A), (B) SiC-W/SN(B).

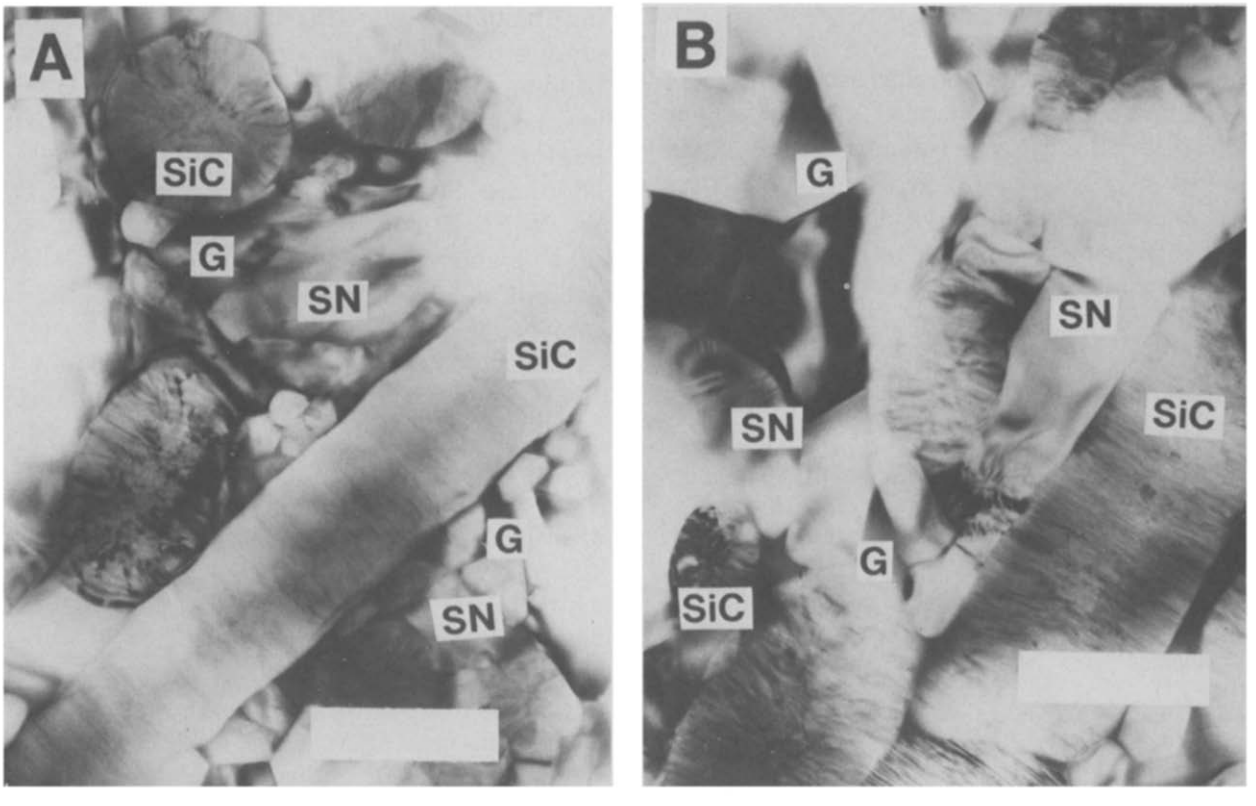

Fig. 3. Transmission electron micrographs of SiC-W/SN composites showing SiC-whiskers and β-Si_3N_4 grains (bar = 1 μm). (A) SiC-W/SN(A), (B) SiC-W/SN(B).

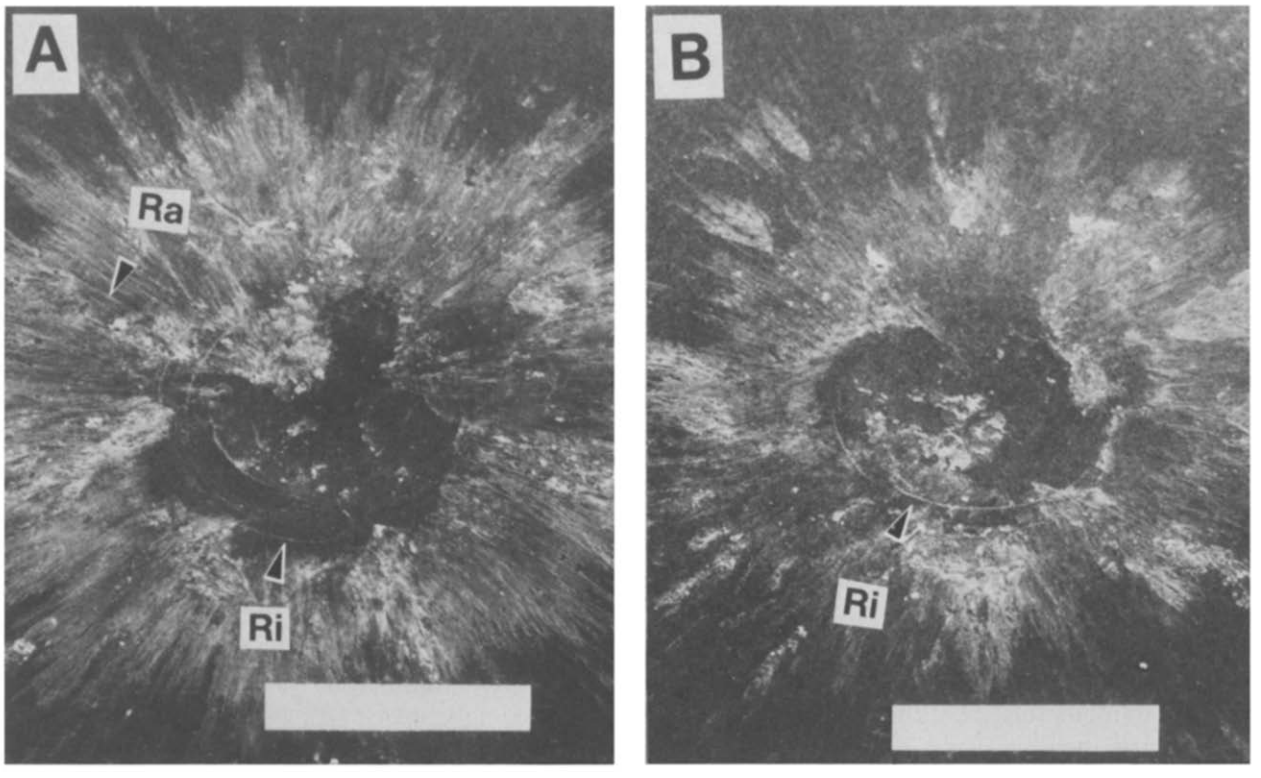

Fig. 4. Scanning electron micrographs of surface damage morphologies near the impact sites at 320 ± 10 m/s impact velocity (bar = 500 μm; Ri, ring crack; Ra, radial crack). (A) SiC-W/SN(A), (B) SiC-W/SN(B).

3.2 Post-impact evaluations

Figure 4(A) and (B) show typical macroscopic surface damage morphologies of the two composites at the impact velocity of 320 ± 10 m/s. The SiC-W/SN(A) composite displays a series of concentric ring cracks (Ri), radial cracks (Ra), a crater and some fragments of the PSZ sphere. The SiC-W/SN(B) composite shows only concentric ring cracks and a crater. Judging from this damage morphology, SiC-W/SN(A) displays elastic/plastic response behavior, whereas SiC-W/SN(B) exhibits purely elastic response. Thus, these two composite exhibit different impact responses. The subsurface crack morphologies are expected to differ also. Considering the ratio of the target hardness to the projectile hardness (Ht/Hp), however, as shown for each specimen in Table 2, these two composites should both fall into the elastic response range ($Ht/Hp > 1$, $Ht/Hp > 1{\cdot}2$).[10,12] Therefore, the subsurface cracks under the impact sites should be further examined.

As the first step of this examination, the residual strengths of the impacted specimens were measured using a four-point bending test. The results are shown in Fig. 5. Although SiC-W/SN(A) exhibits distinct strength degradation at an impact velocity of only 150 m/s, SiC-W/SN(B) does not exhibit serious strength degradation, until 290 m/s. The critical impact velocity for strength degradation is V_c, which for composite SiC-W/SN(B) is in good agreement with a previous report.[13] However, V_c does not agree for SiC-W/SN(A), which is made from thermally decomposed $Si(NH)_2$ powder.

After examining the strength degradation behavior, the fracture surfaces of broken cross-sections were examined to determine the type of cracks initiated beneath the impact site. Examples for each specimen are shown in Fig. 6(A) to (C). Figure 6(A) shows a cone crack, which is the cause of strength degradation in the SiC-W/SN(A) composite at a low impact velocity. A Hertzian cone crack[12,13,19] is also initiated (Fig. 6(B) at a

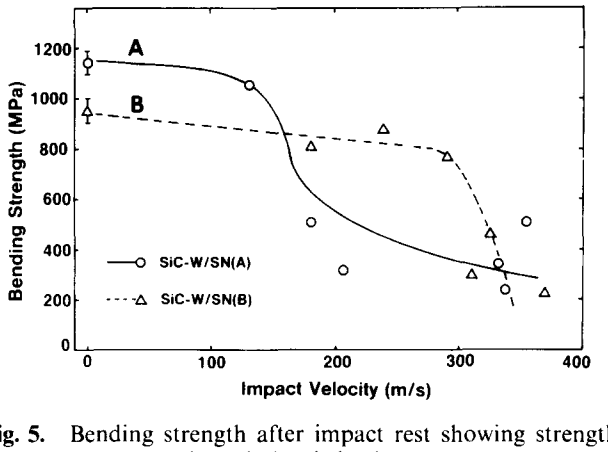

Fig. 5. Bending strength after impact rest showing strength degradation behaviors.

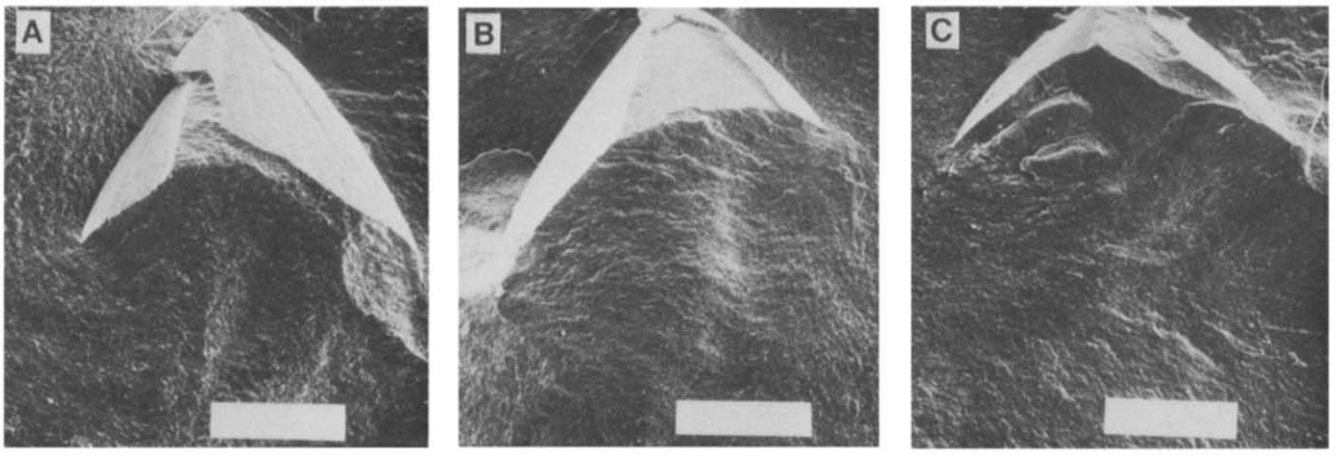

Fig. 6. Fracture surfaces showing Hertz cone crack initiation by impact (bar = 500 μm). (A) SiC-W/SN(A) (V = 181 m/s); (B) SiC-W/SN(A) (V = 331 m/s); (C) SiC-W/SN(B) (V = 324 m/s).

sphere impact velocity of above V_c. However, SiC-W/SN(B) composites do not display any cracks until the impact velocity reaches or exceeds 290 m/s. At these velocities, vary cone cracks are initiated (Fig. 6(C)), immediately resulting in the sudden decrease of the bending strength. Therefore, the dominant impact response behavior of these two materials, ceramic composite was seen to be an elastic response, even though a small crater was created at the impact site. Radial cracks at the surface may have been produced by structural delamination of the plates of needle-like β-Si_3N_4 and SiC-whiskers which occurred during the hot-pressing process.[13]

The hardness value has been defined as an elastic/plastic parameter in the literature.[20] Using the hardnesses of the these two ceramic composite materials, phenomenological analyses were attempted. Shockey *et al.*[10] showed that target response behavior changes from an elastic one to an elastic/plastic one with a decrease in the ratio of the hardness of the target to the hardness of the projectile particle (Ht/Hp). Calculations show that SiC-W/SN(A) has a Ht/Hp ratio of 1·5 and the SiC-W/SN(B) a ratio of 1·35, These ratios are in agreement with literature data.[10,12] This indicates that the behavior of SiC-W/SN(A) should be more elastic than that of SiC-W/SN(B).

Contact behavior can be strongly influenced by the microstructure consisting of a mixture of needle-like β-Si_3N_4 grains, a glass phase and SiC-whiskers. In the Si_3N_4 powder oxygen and carbon contents (which are thought to be in the form of SiO_2 and SiC, respectively) are reported to influence the microstructural development of the matrix material.[7,8] The nitrided silicon powder has a higher oxygen content, but less carbon than the thermally decomposed $Si(NH)_2$ powder (see Table 1). This higher oxygen level and lower carbon level make it easier to produce the glass phase or layer with Y_2O_3 and Al_2O_3 between the Si_3N_4 grains, resulting in a higher sinterability,[8] but also a less rigid structure. This microstructure, achieved through the sintering process of silicon nitride powders, which has a high oxygen content and less carbon provides the resistance to crack initiation caused by localized stresses upon point indentation. Figures 7 and 8

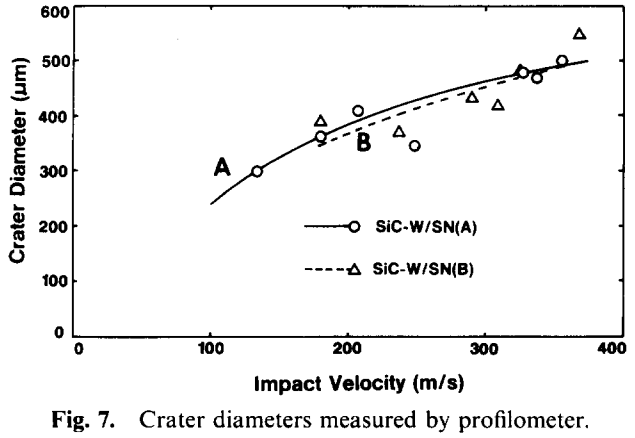

Fig. 7. Crater diameters measured by profilometer.

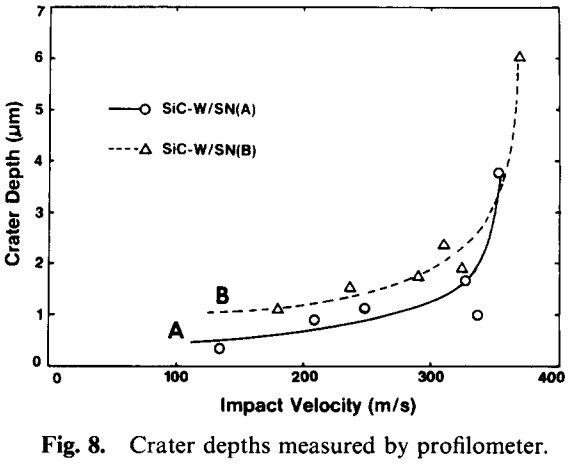

Fig. 8. Crater depths measured by profilometer.

show crater diameters and depths for the specimens. In Fig. 7, little difference is seen in the crater diameters, but the SiC-W/SN(A) composites exhibit a shallower crater depth, which confirm that SiC-W/SN(A) should have an elastic response behavior. This difference in the crater depth results from the microstructural differences.

4 Summary

Two types of SiC-whisker/silicon nitride matrix composites were produced by hot-pressing. One composite was made from nitrided silicon powder and the other from thermally decomposed $Si(NH)_2$ powder. After investigating the mechanical properties and microstructures of these materials, impact tests were conducted to evaluate their damage morphologies and strength degradation.

These composites showed elastic behavior as their dominant response behavior. The SiC-W/SN composite made from nitrided silicon powder displayed lower hardness, which resulted in higher resistance to dynamic Hertzian cone crack initiation and extension upon spherical impact. On the other hand, although the SiC-W/SN composites made from thermally decomposed $Si(NH)_2$ powder displayed higher bending strength and higher hardnesses, they showed less resistance to crack initiation and strength degradation upon spherical impact. The reason for this is considered to be that the nitrided silicon powder contains a higher oxygen content and lower carbon content and thus yields a less elastic, less rigid microstructure, one which is better able to dissipate energy during impact.

Acknowledgement

The author gratefully acknowledges the review of this manuscript by Dr Richard C. Bradt, Dean of University of Nevada-Reno.

References

1. Richerson, D. W., Evolution in the US of ceramic technology for turbine engines. *Am. Ceram. Soc. Bull.*, **64**(2) (1985) 282–6.
2. Boyd, G. L. & Kreiner, D. M., AGT101/ATTAP ceramic technology. In *Proceedings of the 25th Automotive Technology Development Contractors' Coordination Meeting*. Society of Automotive Engineers, Warrendale, USA, 1988, pp. 101–23.
3. Ueno, K. & Toibana, Y., Mechanical properties of silicon nitride ceramic composite reinforced with silicon carbide whisker. *Yogyo-Kyokaishi*, **91**(11) (1983) 491–7.
4. Shalek, P. D., Petrovic, J. J., Hurley, G. F. & Gac, F. D., Hot-pressed SiC whisker/Si_3N_4 matrix composites. *Am. Ceram. Soc. Bull.*, **65**(2) (1986) 351–6.
5. Buljan, S. T., Baldoni, J. G. & Huckabee, M. L., *Si_3N_4–SiC* composite. *Am. Ceram. Soc. Bull.*, **66**(2) (1987) 347–52.
6. Li, Z. & Bradt, R. C., Micromechanical stresses in SiC-reinforced Al_2O_3 composites. *J. Am. Ceram. Soc.*, **72**(1) (1989) 70–7.
7. Wotting, G. & Ziegler, G., Influence of powder properties and processing conditions on microstructure and mechanical properties of sintered Si_3N_4. *Ceramics International*, **10**(1) (1984) 18–20.
8. Mitomo, Y., Yang, N., Kishi, Y. & Bando, Y., Influence of powder characteristics on gas pressure sintering of Si_3N_4. *J. Mat. Sci.*, **23** (1988) 3413–19.
9. Dao, K. C., Shockey, D. A., Seamon, L., Durran, D. R. & Rowcliffe, D. J., Particle impact damage in silicon nitride. *Annual Reports, Part III*, Office of Naval Research, Contract No. N00014-76-057, May 1979.
10. Shockey, D. A., Erlich, D. C. & Dao, K. C., Particle impact damage in silicon nitride at 1400°C. *J. Mater. Sci.*, **16** (1981) 477–82.
11. Cussio, J. & Fang, H., Impact damage study of silicon nitride. In *Proceedings of the 26th Automotive Technology Development Contractors Coordination Meeting*. Society of Automotive Engineers, Warrendale, PA, USA, 1988.
12. Akimune, Y., Katano, Y. & Matoba, K., Spherical impact damage and strength degradation in silicon nitride for automobile turbocharger rotors. *J. Am. Ceram. Soc.*, **72**(8) (1989) 1422–8.
13. Akimune, Y., Katano, Y. & Matoba, K., Spherical impact damage and strength degradation in SiC-whisker/Si_3N_4 composites. *J. Am. Ceram. Soc.*, **72**(5) (1989) 791–8.
14. Brender, K., Ritter, J. E. & Jakus, K., Strength degradation in polycrystalline alumina due to sharp-particle impact damage. *J. Am. Ceram. Soc.*, **71**(12) (1988) 1154–8.
15. Weibull, W., A statistical distribution function of wide applicability. *J. Appl. Mech.*, **18** (1951) 293–7.
16. Lawn, B. R. & Fuller, E. R., Equilibrium penny-like cracks in identation fracture. *J. Mater. Sci.*, **10**(12) (1975) 2016–24.
17. Sarin, V. K. & Ruhle, M., Microstructural studies of ceramic matrix composites. *Composites* **18**(2) (1987) 129–34.
18. Hsueh, C. H., Becher, P. F. & Angelini, P., Effect of interfacial films on thermal stresses in whisker-reinforced ceramics. *J. Am. Ceram. Soc.*, **71**(11) (1988) 929–33.
19. Hertz, H. R., *Hertz's Miscellaneous Papers*. MacMillan, London, 1896, Chapters 5 and 6.
20. Lawn, B. R. & Howes, V. R., Elastic recovery at hardness indentation. *J. Mat. Sci.*, **16** (1981) 2745–52.